Electromagnetic Waves in a Cylindrical Waveguide with Infinite or Semi-Infinite Wall Corrugations

S. LENNART G. LUNDQVIST

Abstract — **The electromagnetic waves inside a circular waveguide having a periodically varying radius with corrugations of infinite or semi-infinite extent are considered. The infinitely corrugated waveguide is investigated by use of the null field approach, and some plots of the axial wavenumbers are presented. For a junction between a straight and a corrugated waveguide, the reflection and transmission coefficients are determined by mode matching, and some computations of these reflection coefficients are also given.**

I. Introduction

In the first part of the present paper we investigate the propagating and nonpropagating electromagnetic modes in a circular waveguide with a periodically varying radius and a perfectly conducting wall. The fields inside the waveguide and the axial wavenumbers are determined using the null field approach. The same approach has previously been used by Boström [1] to determine the stopband and passband structure for the same problem. Lundqvist and Boström [2] have considered the corresponding acoustic problem with waves in ducts with infinite, semi-infinite, or finite wall corrugations and Sandström [3] has considered the two-dimensional problem with modes in corrugated waveguides.

For small wall corrugations, further references are given in the review article by Asfar and Nayfeh [4]. For the problem under consideration, Kheifets [5] has developed a method for finding approximate analytic solutions for slowly varying boundaries. For small wall corrugations, Asfar and Nayfeh [6] have proved that modes become exponentially decreasing when they propagate in opposite directions and their axial wavenumbers differ by a multiple of the wavenumber of the waveguide.

From the numerical results below, it is observed that the axial wavenumbers never coincide as the frequency varies, except possibly at isolated frequency points. This property imposes some predictable features on the solutions when the mode is exponentially decreasing along the waveguide. Some of these features have been proved for the Hill equation and noticed in other periodic structures (cf. the review article by Elachi [7]).

Manuscript received September 11, 1987; revised June 12, 1987. This work was supported in part by the National Swedish Board for Technical Development.

The author is with the Institute of Theoretical Physics, S-412 96 Göteborg, Sweden

IEEE Log Number 8717591.

In the second part of this paper we compute the reflection and transmission matrices for a junction between a straight and a corrugated waveguide. From these matrices, and a building-block method, it is a simple matter to compute the reflection and transmission for a finite corrugated part in an otherwise straight waveguide (cf. [2] and [8]).

II. The Modes in a Corrugated Waveguide

Consider a cylindrical waveguide with a periodically varying circular cross section. In cylindrical coordinates the radius ρ thus varies along the waveguide axis z as $\rho = R(z)$, where $R(z)$ is periodic in z with period $2b$. The wall corrugation is assumed to be even and the time harmonic dependence $e^{-i\omega t}$ is assumed and suppressed. For an isotropic, homogeneous, and lossless medium inside the waveguide, the electric field $\vec{E}$ (or the magnetic field $\vec{H}$) satisfies the homogeneous vector Helmholtz equation

$$\nabla \times \nabla \times \vec{E} - k^2 \vec{E} = 0 \tag{1}$$

where the wavenumber $k = \omega/c$ is real and c is the velocity of light. The wall of the waveguide is assumed to be perfectly conducting:

$$\hat{n} \times \vec{E}(\vec{r}) = 0 \tag{2}$$

where $\hat{n}$ is the outward-pointing unit normal.

As in the case of Boström [1], the even modes in the corrugated waveguide can be defined as

$$\vec{w}^{\pm}_{\tau m j}(\vec{r}) = \sum_{\tau'=1}^{2} \sum_{n=-\infty}^{\infty} \alpha_{\tau m j n \tau'} \operatorname{Re} \vec{\chi}_{\tau' m}\left(\pm h_{\tau m j} \pm n\pi/b; \vec{r}\right) \tag{3}$$

where

$$\operatorname{Re} \vec{\chi}_{\tau m}(h; \vec{r}) = \sqrt{\frac{\epsilon_m}{8\pi}} \frac{k}{q} (k^{-1} \nabla \times)^{\tau} \left\{ \hat{z} J_m(qp) e^{ihz} \left(\delta_{\tau 1} \cos(m\phi) + \delta_{\tau 2} \sin(m\phi)\right)\right\} \tag{4}$$

with j the mode number, $\tau = 1,2$ for TE and TM waves, $m = 0,1,2,\cdots$, $\epsilon_0 = 1$ and $\epsilon_m = 2$ for $m \neq 0$, and $q = (k^2 - h^2)^{1/2}$ with $\operatorname{Im}(q) \geq 0$. The + (−) denotes modes that propagate in the positive (negative) z direction and J_m is the Bessel function of order m. For the odd-mode solutions, the Kronecker deltas just switch places. The triplet

0018-9480/88/0100-0028$01.00

τmj corresponds to the usual enumeration of waveguide modes, so that $\tau=1$, $m=1$, and $j=2$ designates the TE_{12} mode. Note that we maintain the TE and TM names in spite of the fact that the actual modes in a corrugated waveguide are not of the transverse electric or magnetic type.

The infinite set of constants $\alpha_{\tau mjn\tau'}$ is determined from (apart from the normalization which is discussed in the next section)

$$\sum_{\tau''=1}^{2}\sum_{n=-\infty}^{\infty} Q^{(m)}_{\tau' n',\tau'' n}(h_{\tau mj})\alpha_{\tau mjn\tau''}=0 \tag{5}$$

and the axial wavenumbers $h_{\tau mj}$ are given by the values where the Q matrix is singular:

$$\det\{Q^{(m)}_{\tau' n',\tau n}(h)\}=0. \tag{6}$$

The elements of the Q matrix are given by

$$Q^{(m)}_{\tau' n',\tau n}(h)=\frac{k}{b}\int_0^{2\pi}d\phi\int_{-b}^{b}\operatorname{Re}\vec{\chi}_{\tau' m}(h+n'\pi/b,R(z),\phi,z)\cdot\vec{G}_{\tau m}(h+n\pi/b,R(z),\phi,z)R(z)\frac{dz}{n_\rho} \tag{7}$$

where $n_\rho=\hat{n}\cdot\hat{\rho}$ and

$$\vec{G}_{\tau m}(h;\vec{r})=k^{-1}\hat{n}\times(\nabla\times\operatorname{Re}\vec{\chi}(h;\vec{r})). \tag{8}$$

For this particular choice of $\vec{G}_{\tau m}$ the modes (3) are valid in the whole waveguide (cf. Millar [9]). Other forms of $\vec{G}_{\tau m}$ are possible, corresponding to different expansions of the surface field, but these expansions are valid only on the surface. An expansion of the surface field in trigonometric functions, for instance, gives (for even modes)

$$\vec{G}_{\tau m}(h;\vec{r})=e^{ihz}(\hat{\phi}\cos(m\phi)\delta_{\tau 1}+\hat{n}\times\hat{\phi}\sin(m\phi)\delta_{\tau 2}). \tag{9}$$

From (3) it is apparent that if h satisfies (6), then $h+p\pi/b$ (for any integer p) is also a solution. Thus, to determine a mode unambiguously, both the axial wavenumber $h_{\tau mj}$ and all constants $\alpha_{\tau mjn\tau'}$ are required. If one solution corresponds to an axial wavenumber h, then the complex conjugate of h is also associated with a solution. If we change z for $-z$ (a solution is equally a solution when it propagates in the opposite direction for an even periodic boundary) we see that $-h$ gives a solution. Thus if $\operatorname{Re}(h)\neq p\pi/b-\operatorname{Re}(h)$, for any integer p, and $\operatorname{Im}(h)\neq 0$, four different solutions exist corresponding to h, h^*, $-h$, and $-h^*$.

III. Waveguides with Semi-Infinite Wall Corrugations

We let the even electric modes be defined as in (3) in the previous section and we now fix the normalization. We impose a normalization that gives the modes unit energy flux along the waveguide for propagating modes; i.e., we set the z component of the complex Poynting vector, integrated over the cross section at $z=0$, equal to unity (for simplicity we now suppress the τ and m indices):

$$i\int_{z=0}\vec{w}_j^{\pm}\times(\nabla\times\vec{w}_j^{\pm})^*\cdot d\vec{s}=1 \tag{10}$$

and from a numerical point of view they are "almost orthonormal," i.e.,

$$i\int_{z=0}\vec{w}_{j'}^{\pm}\times(\nabla\times\vec{w}_j^{\pm})^*\cdot d\vec{s}=\begin{cases}1 & \text{for } j=j'\\ \epsilon & \text{for } j\neq j'\end{cases} \tag{11}$$

where ϵ is of order 10^{-3}. Huang [10] has studied modes in waveguides that are "almost orthonormal."

The even modes in the straight waveguide are defined by

$$\vec{v}^{\pm}_{\tau mj}(\vec{r})=\operatorname{Re}\vec{\chi}_{\tau m}(\pm H_{\tau mj};\vec{r}) \tag{12}$$

with $J'_m(eQ_{\tau mj})=0$ for $\tau=1$ and $J_m(eQ_{\tau mj})=0$ for $\tau=2$. where e is the radius of the straight waveguide and $Q_{\tau mj}=(k^2-H^2_{\tau mj})^{1/2}$ with $\operatorname{Im}Q_{\tau mj}\geq 0$. We impose the normalization (10) also on these modes and they are both complete and orthogonal.

Consider now a junction between a straight waveguide for $z<0$ and a corrugated one for $z>0$. If we assume an incoming mode in the straight waveguide, the solution in the whole waveguide can be written as

$$\vec{E}(\vec{r})=\begin{cases}\vec{v}_j^{+}+\sum_{j'}R^{11}_{jj'}\vec{v}_{j'}^{-}, & z<0\\ \sum_{j'}T^{12}_{jj'}\vec{w}_{j'}^{+}, & z>0\end{cases} \tag{13}$$

where R^{11} and T^{12} are the reflection and transmission matrices. If we assume no discontinuity of the medium inside the waveguide, the continuity of the transverse part of the electric and magnetic fields at $z=0$ gives

$$\hat{z}\times\vec{v}_j^{+}+\sum_{j'}R^{11}_{jj'}\hat{z}\times\vec{v}_{j'}^{-}=\sum_{j'}T^{12}_{jj'}\hat{z}\times\vec{w}_{j'}^{+} \tag{14a}$$

$$\hat{z}\times(\nabla\times\vec{v}_j^{+})+\sum_{j'}R^{11}_{jj'}\hat{z}\times(\nabla\times\vec{v}_{j'}^{-})=\sum_{j'}T^{12}_{jj'}\hat{z}\times(\nabla\times\vec{w}_{j'}^{+}). \tag{14b}$$

To solve for the matrices R^{11} and T^{12}, we project (14a) on the system $\{\nabla\times\vec{v}_{j''}^{+}\}$ and (14b) on $\{\vec{v}_{j''}^{+}\}$ and use the orthogonality of $\{\vec{v}_j^{+}\}$:

$$\begin{aligned}\delta_{jj''}+R^{11}_{jj''}&=\sum_{j'}T^{12}_{jj'}M_{j'j''}\\ \delta_{jj''}-R^{11}_{jj''}&=\sum_{j'}T^{12}_{jj'}N_{j'j''}\end{aligned} \tag{15}$$

where

$$\begin{aligned}M_{j'j''}&=\int_{z=0}[\vec{w}_{j'}^{+}\times(\nabla\times\vec{v}_{j''}^{+})]\cdot d\vec{s}\\ N_{j'j''}&=\int_{z=0}[(\nabla\times\vec{w}_{j'}^{+})\times\vec{v}_{j''}^{+}]\cdot d\vec{s}.\end{aligned} \tag{16}$$

Accordingly we get

$$\begin{aligned}R^{11}_{jj'}&=2\sum_{j''}(M_{jj''}+N_{jj''})^{-1}M_{j''j'}+\delta_{jj'}\\ T^{12}_{jj'}&=2(M_{jj'}+N_{jj'})^{-1}.\end{aligned} \tag{17}$$

All the matrix elements of M and N can be computed analytically. If we introduce the restriction $m=1$ and suppress the m value, in order to make the notation simpler, we get (apart from the normalization factors)

$$M_{jj'} = M^{(m=1)}_{\tau j,\tau' j'} = \frac{\pi}{2} \sum_{n=-\infty}^{\infty} \sum_{\tau''=1}^{2} \alpha_{\tau jn\tau''} \Big\{ \xi_{\tau jn\tau' j'} \big(\delta_{\tau' 1}\delta_{\tau'' 1} H_{\tau' j'} - \delta_{\tau' 2}\delta_{\tau'' 2} h_{\tau jn} k / H_{\tau' j'} \big) + \zeta_{\tau jn\tau' j'} \big(\delta_{\tau' 1}\delta_{\tau'' 2} H_{\tau' j'} h_{\tau jn}/k + \delta_{\tau' 2}\delta_{\tau'' 1} k \big) \Big\}$$

$$N_{jj'} = N^{(m=1)}_{\tau j,\tau' j'} = \frac{\pi}{2} \sum_{n=-\infty}^{\infty} \sum_{\tau''=1}^{2} \alpha_{\tau jn\tau''} \Big\{ \xi_{\tau jn\tau' j'} \big(\delta_{\tau' 1}\delta_{\tau'' 1} h_{\tau jn} - \delta_{\tau' 2}\delta_{\tau'' 2} H_{\tau' j'} \big) + \zeta_{\tau jn\tau' j'} \big(\delta_{\tau' 1}\delta_{\tau'' 2} k + \delta_{\tau' 2}\delta_{\tau'' 1} H_{\tau' j'} h_{\tau jn}/k \big) \Big\} \tag{18}$$

where

$$\zeta_{\tau jn\tau' j'} = \begin{cases} \big(q^2_{\tau jn} - Q^2_{\tau' j'} \big)^{-1} \big\{ q_{\tau jn} e J_1(q_{\tau jn} e) J_0(Q_{\tau' j'} e) - Q_{\tau' j'} e J_0(q_{\tau jn} e) J_1(Q_{\tau' j'} e) + q_{\tau jn} e J_3(q_{\tau jn} e) J_2(Q_{\tau' j'} e) - Q_{\tau' j'} e J_2(q_{\tau jn} e) J_3(Q_{\tau' j'} e) \big\} \\ \qquad \text{if } q^2_{\tau jn} \neq Q^2_{\tau' j'} \\ e^2 J_0^2(Q_{\tau jn} e) + J_1(Q_{\tau jn} e) \left(e^2 - \dfrac{2}{Q^2_{\tau jn}} \right) \\ \qquad \text{if } q^2_{\tau jn} = Q^2_{\tau' j'} \end{cases} \tag{19}$$

$$\xi_{\tau jn\tau' j'} = 2i \frac{J_1(q_{\tau jn} e) J_1(Q_{\tau' j'} e)}{q_{\tau jn} Q_{\tau' j'}}. \tag{20}$$

We have used the notation

$$h_{\tau jn} = h_{\tau j} + n\pi/b$$

$$q_{\tau jn} = \big(k^2 - h^2_{\tau jn} \big)^{1/2}, \qquad \operatorname{Im} q_{\tau jn} \geq 0. \tag{21}$$

If we instead assume an incoming mode in the corrugated waveguide, the solution in the whole waveguide can be written as

$$\vec{E}(\vec{r}) = \begin{cases} \vec{w}_j^- + \sum_{j'} R^{22}_{jj'} \vec{w}^+_{j'}, & z > 0 \\ \sum_{j'} T^{21}_{jj'} \vec{v}^-_{j'}, & z < 0. \end{cases} \tag{22}$$

The continuity conditions and the same projections determine R^{22} and T^{21} in a way similar to (17). From reciprocity it follows that R^{11} and R^{22} are symmetric matrices and that $T^{21}_{jj'} = T^{12}_{j'j}$. These features are used as a check.

IV. Numerical Results and Discussion

In the numerical computations we have used a waveguide where the radius of the wall, $R(z)$, is given by

$$R(z) = a + d\cos\left(\frac{z\pi}{a}\right). \tag{23}$$

The mean diameter is thus equal to the wavelength of the wall corrugations. We further specialize to the case $m=1$ as the fundamental mode TE_{11} has this m value.

TABLE I
Cut-on and Resonance Frequencies for an Infinitesimally Corrugated Waveguide, together with the Resonating Modes, Propagation in the Opposite or Same Direction, and the Resulting Interference Type, for a Waveguide with Mean Diameter Equal to the Period of the Wall

ka	modes	directions	type
1.841	TE_{11}	—	cut-on
2.420	$TE_{11}TE_{11}$	opposite	stopband
3.641	$TE_{11}TE_{11}$	opposite	stopband
3.832	TM_{11}	—	cut-on
3.838	$TE_{11}TM_{11}$	same	crossover
4.141	$TM_{11}TM_{11}$	opposite	stopband
4.440	$TE_{11}TM_{11}$	opposite	stopband
4.955	$TM_{11}TM_{11}$	opposite	stopband
5.059	$TE_{11}TE_{11}$	opposite	stopband
5.331	TE_{12}	—	cut-on
5.367	$TM_{11}TE_{12}$	same	crossover
5.454	$TE_{11}TE_{12}$	opposite	stopband
5.558	$TE_{12}TE_{12}$	opposite	stopband
5.622	$TE_{11}TM_{11}$	opposite	stopband
5.711	$TM_{11}TE_{12}$	opposite	stopband
5.852	$TE_{11}TE_{12}$	same	crossover
6.078	$TM_{11}TM_{11}$	opposite	stopband
6.188	$TE_{12}TE_{12}$	opposite	stopband
6.315	$TE_{11}TE_{12}$	opposite	stopband
6.544	$TE_{11}TE_{11}$	opposite	stopband
6.655	$TE_{12}TM_{11}$	opposite	stopband
6.982	$TE_{11}TM_{11}$	opposite	stopband
7.016	TM_{12}	—	cut-on

For the straight cylinder, the frequency points where two axial wavenumbers differ by a multiple of π/a (the wavenumber of the corrugated wall) are presented in the first column of Table I. In the second column the interacting modes are labeled and the third column states if the modes propagate in the same or opposite directions. Table I also shows the type of interference; stopband if the resulting imaginary part differs from zero; otherwise crossover. This last column is determined by inspection of the numerical data. The resulting resonances follow a simple scheme: two modes propagating in the same (opposite) direction give rise to a crossover (stopband). For moderate undulations this has been proved by Asfar and Nayfeh [6] for interferences between TE–TE modes and TM–TM modes. We note that the results of Table I (and also of Figs. 1–4 below) are not in close accordance with those of Boström [1]. However, this is due to a programming error in [1] (see [11]).

In Figs. 1 and 3 the real part of the axial wavenumber is plotted as a function of frequency and in Figs. 2 and 4 the corresponding imaginary part is presented, for corrugations $d/a = 0.10$ and 0.20, respectively. In all of the figures the lowest mode, TE_{11}, is drawn with a solid line, the TM_{11} mode with a dashed line, the TE_{12} mode with a dash-dotted line, and the TM_{12} mode with a dotted line.

The crossover between the TE_{11} and TM_{11} modes around $ka = 3.83$ is easily recognized for $d/a = 0.10$ and, as for the crossover interference between the TE_{11} and the TE_{12} modes around $ka = 5.95$, it has been plotted with some overlap. In Figs. 3 and 4 ($d/a = 0.20$) these crossover resonances have disappeared. The crossover between the

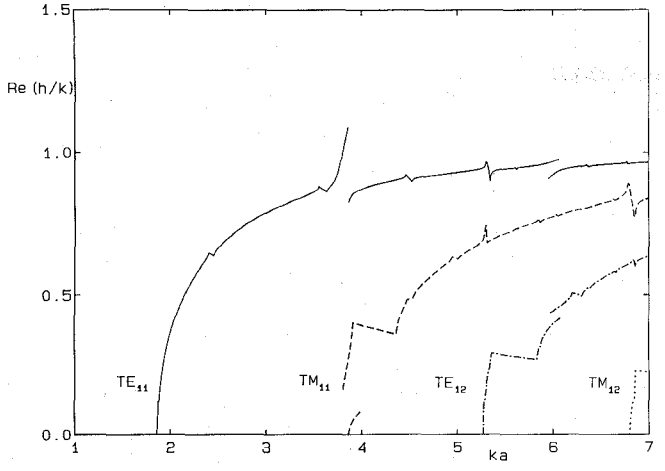

Fig. 1. The real part of the axial wavenumber as a function of frequency for corrugation $d/a = 0.10$.

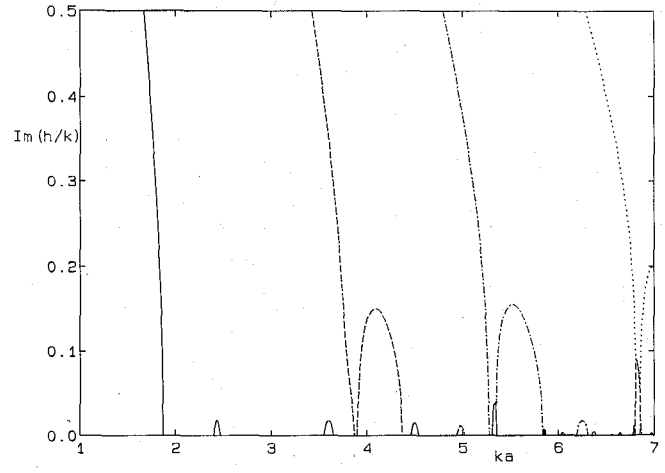

Fig. 2. The same as Fig. 1 but for the imaginary part of the axial wavenumber.

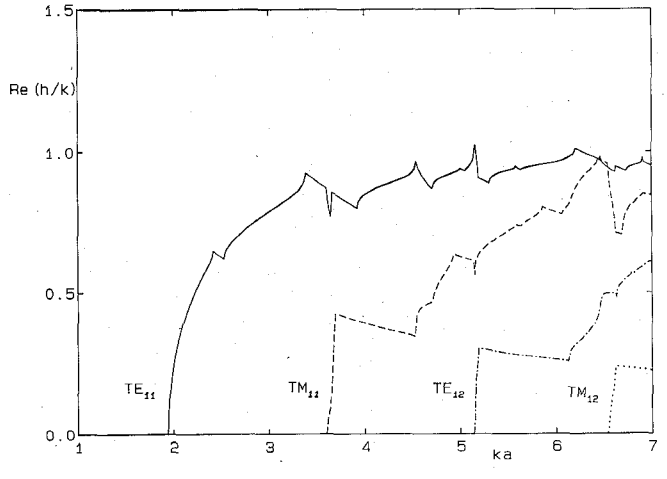

Fig. 3. The real part of the axial wavenumber as a function of frequency for corrugation $d/a = 0.20$.

TE_{12} and TM_{11} modes at $ka = 5.33$ (cf. Table I) has already disappeared in Figs. 1 and 2. The development between the two states can be interpreted as a result of degeneracy at a point for the axial wavenumber. As the corrugation increases from $d/a = 0.10$ to 0.20, the stopband initially at $ka = 3.64$ broadens and a point is reached

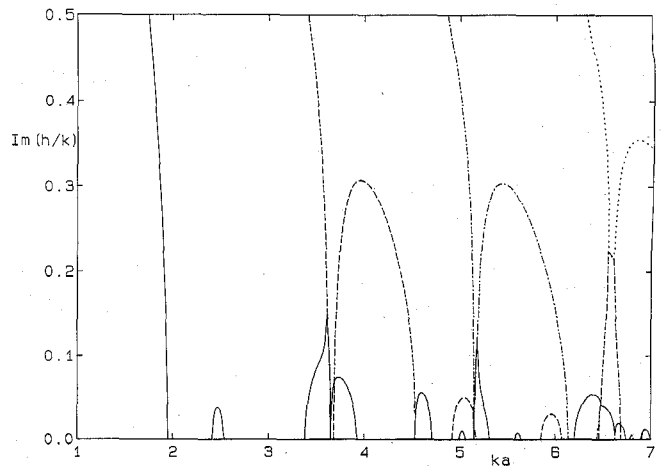

Fig. 4. The same as Fig. 3 but for the imaginary part of the axial wavenumber.

where the imaginary part of the TE_{11} mode coincides with the imaginary part of the cutoff TM_{11} mode. At this point the real parts of the axial wavenumbers are also identical (they only differ by an immaterial π/a). A degeneration (double) point has occurred and the crossover interference takes place here. for the crossover interference between TM_{11} and TE_{12}, the double point has just emerged for $d/a = 0.10$ and occurs approximately at the cut-on frequency for the TE_{12} mode; it is recognizable as the top of the peak at $ka = 5.30$ for the TM_{11} mode.

In all the stopbands presented, the real parts of the axial wavenumbers satisfy simple relations. For an interaction between one mode and itself, traveling in the opposite direction, the sum of the absolute values of the real parts of the axial wavenumbers equals a multiple of the wavenumber of the cylinder: $\mathrm{Re}(h_1 + h_1) = \pi p/a$ (note that in the figures we have plotted h/k). The interferences where $p = 1$ in Fig. 3 are located around $ka = 2.48$ for the TE_{11} mode, $ka = 4.15$ for the TM_{11} mode, $ka = 5.70$ for the TE_{12} mode, and $ka = 6.80$ for the TM_{12} mode. For $p = 2$ the interferences occur around $ka = 3.50$ and 3.75 for the TE_{11} mode and $ka = 5.00$ for the TM_{11} mode. For $p = 3$ the frequency domains are situated around $ka = 5.00$ and 5.25 for the TE_{11} mode and at $ka = 6.00$ and $ka = 6.65$ for the TM_{11} mode. Finally, for $p = 4$, they are at $ka = 6.30$ and $ka = 6.70$ for the TE_{11} mode.

In a stopband due to an interference between two different modes, the same relation holds, $\mathrm{RE}(h_1 + h_2) = \pi p/a$ and $\mathrm{Im}(h_1) = \mathrm{Im}(h_2)$, but with the extra condition $\mathrm{Re}(h_1) \neq \pi p/a \neq \mathrm{Re}(h_2)$. All stopbands not enumerated above are of this type. For the TE_{11} and TM_{11} mode this type of interference occurs in Fig. 3 around $ka = 3.63$ (at the dip for the TE_{11} mode), $ka = 4.55$, 5.60, and 6.95. The coincidence of the imaginary parts is sometimes hard to observe in the figures, but could always be recognized by the appearance of the real parts and the fact that outside the stopbands the real parts of all the axial wavenumbers always increase which increasing frequency.

Both types of interference conditions preserve the total number of axial wavenumber solutions that exists outside

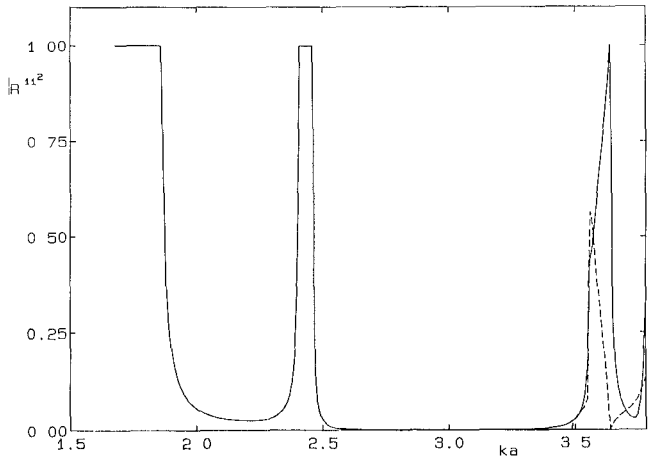

Fig. 5 The reflection coefficients for the reflected modes TE_{11} (solid line) and TM_{11} (broken line) for the lowest mode, TE_{11}, impinging on a junction between a sinusoidally corrugated waveguide with $d/a = 0.10$ joined at its largest cross section to a straight waveguide.

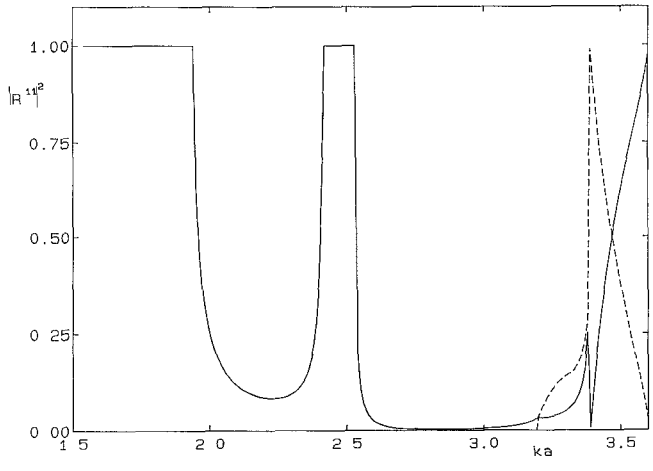

Fig. 6 The same as Fig. 5 but for $d/a = 0.20$

the stopband. In a stopband due to an interference of a mode with itself, two different axial wavenumber solutions exist (h_1 and $-h_1$, since $h_1^* = -h_1 + p\pi/a$ for some integer p) corresponding to two solutions outside (h_1 and $-h_1$). For the other stopbands four solutions exist inside the stopband (h_1, $-h_1$, h_1^* and $-h_1^*$), exactly as many as outside the stopband (corresponding to h_1, $-h_1$, h_2 and $-h_2$).

In the opposite way around, if we impose that the number of possible axial wavenumber solutions should be equal inside and outside a stopband, the interference conditions above follow. It is observed in several periodic contexts (for instance, the Hill equation [2], [3], [7]) that the real part of the axial wavenumber is constant in stopbands. This can thus be interpreted as a conservation restriction on the number of solutions.

For a more detailed discussion of the axial wavenumber dependence as the corrugation increases, we refer the reader to Lundqvist and Boström [2], where the analogous acoustic case is treated.

In Figs. 5 and 6 the reflected energies ($|R^{11}|^2$) are plotted for an incoming TE_{11} mode in a straight cylinder impinging upon a junction between a straight and a corrugated waveguide, for corrugations $d/a = 0.10$ and 0.20, respectively. To make comparisons with Figs. 1 to 4 easier, the energies are plotted against ka, where a is the mean radius in the corrugated waveguide. The junction is situated at the maximum radius in the corrugated waveguide; the radius in the straight waveguide is thus $e = a + d$. Three nonpropagating modes are used in the computations, but only the modes that are cut on for the straight cylinder are plotted. We plot the reflected energy in the TE_{11} mode with a solid line and the reflected energy in the TM_{11} mode with a dashed line.

Around $ka = 2.45$ in Figs. 5 and 6, and below the cut-on of the TE_{11} mode in the corrugated waveguide, no mode is propagating in the corrugated waveguide and accordingly total reflection occurs. For $ka > 3.484$ for $d/a = 0.10$ and $ka \geqslant 3.193$ for $d/a = 0.20$, two modes are propagating in the straight waveguide. In the stopband around $ka = 3.64$ in Figs. 5 and 6, the sum of the reflected energies from the two propagating modes equals one, with an error less than 10^{-3}.

At higher frequencies the reflection coefficients become very irregular and since the accuracy decreases with increasing frequency and with the number of cut-on modes in the corrugated waveguide, in Figs. 5 and 6 we plot only the frequency range with at most one mode cut on in the corrugated part.

In conclusion, both propagating and nonpropagating modes in a sinusoidally corrugated waveguide have been computed by using the null field approach. The junction between a straight and a corrugated waveguide has also been considered and as in the analogous acoustic case [2] it would be easy to compute the reflection and transmission from a finite corrugated section.

Acknowledgment

The author wishes to thank Prof. A. Boström for his guidance and for reading the manuscript.

References

[1] A. Boström, "Passbands and stopbands for an electromagnetic waveguide with a periodically varying cross section," *IEEE Trans. Microwave Theory Tech.*, vol. MTT-31, pp. 752–756, Sept. 1983.

[2] L. Lundqvist and A. Boström, "Acoustic waves in a cylindrical duct with infinite, half-infinite, or finite wall corrugations," *J. Sound Vibration*, to be published.

[3] S.-E. Sandström, "Stopbands in a corrugated parallel plate waveguide," *J. Acoust. Soc. Amer.*, to be published.

[4] O R. Asfar and A. H. Nayfeh, "The application of the method of multiple scales to wave propagation in periodic structures," *SIAM Rev.*, vol. 25, pp. 455–480, 1983.

[5] S. A. Kheifets, "Electromagnetic fields in an axial symmetric waveguide with variable cross section," *IEEE Trans. Microwave Theory Tech.*, vol. MTT-29, pp. 222–229, Mar. 1981.

[6] O. R. Asfar and A. H. Nayfeh, "Circular waveguide with sinusoidally perturbed wall," *IEEE Trans. Microwave Theory Tech.*, vol. MTT-23, pp. 728–734, 1975.

[7] C Elachi, "Waves in active and passive periodic structures: A review," *Proc IEEE*, vol. 64, pp. 1666–1698, 1976.

[8] A Boström and B Nilsson, "Acoustics of an obstacle inside a reactive silencer," *J Sound Vibration*, vol. 87, pp. 603–619, 1983.

[9] R. F. Millar, "The Rayleigh hypothesis and a related least-squares solution to scattering problems for periodic surfaces and other scatterers," *Radio Sci.*, vol. 8, pp. 785–796, 1973.
[10] H. Huang, "General theory of nonconventional waveguides for long-distance transmission," *Scientia Sinica*, vol. 11, pp. 761–784, 1962.
[11] A. Boström, private communication.

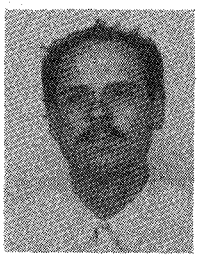

S. Lennart G. Lundqvist was born in Göteborg, Sweden, on May 20, 1953. He received the B.S. degree in mathematics and physics in 1978 and the Ph.D. degree in theoretical physics in 1986, both from the University of Göteborg. His doctoral research was on acoustic and electromagnetic corrugated waveguides with periodically varying cross section.